# Supporting Information

## CdAg Alloy@Polymer dots of Biginelli Polyamide for Highly Sensitive and Selective Recognition of Nerve Agent mimic in an Aqueous and Vapor phase

Manpreet Kaur,[a] Navneet Kaur,*[a] and Narinder Singh*[b]

[a]Department of Chemistry, Panjab University, Chandigarh, India, 160014, E-mail: navneetkaur@pu.ac.in.
[b*]Department of Chemistry, Indian Institute of Technology Ropar (IIT Ropar), Rupnagar, Punjab, 140001, India. E-mail: nsingh@iitrpr.ac.in; Tel: +91-1881242176

**Table of Contents**

**Figure S5**: (A) Stacked FTIR spectra of complex CdAg Alloy@Pdots+DCP and CdAg Alloy@Pdots+DCNP in comparison with CdAg Alloy@Pdots, Pdots only, DCP only and DCNP only. (B) $^{31}P$ NMR of CdAgAlloy@Pdots in presence of increasing equvalents of DCP recorded in $D_2O$ solvent.

**Figure S6:** DLS histogram of CdAgAlloy@PDots+DCP shows average size in range of 124-130 nm.

**Figure S7:** Bar graph showing interference studies of CdAgAlloy@Pdots complex with DCP and DCNP respectively, in presence of other phosphates.

**Figure S8:** Scan rate study at different scan rate (10 mV/S to 250 mV/S) at concentration 22 nM of DCP.

**Figure S9:** pH effect studies of (A) Pdots and (B) CdAg Alloy@Pdots in wide range of pH from 2-11.

**Figure S10:** Absorption spectra of (A) Pdots and (B) CdAgAlloy@Pdots showing no remarkable change after 48h of low power UV-light irradiation.

**Table S2**: Comparison of LOD and studies with reported other sensing materials of DCP and DCNP.

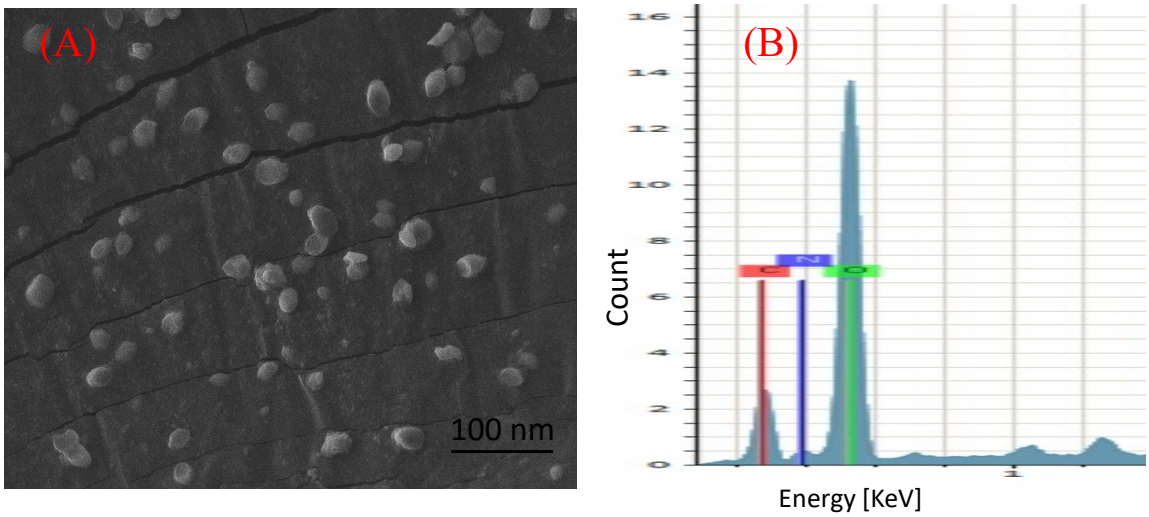


**Figure S1:** (A) SEM image and (B) EDX analysis bar of Pdots respectively.

**Table S1:** Zeta potential values of Pdots.

| **Pdots** | **Zeta Potential (in mV)** | | | **Average Zeta Potential** |
|---|---|---|---|---|
| | Reading 1 | Reading 2 | Reading 3 | |
| | -27.2 mV | -27.4 mV | -28.0 mV | -27.5 mV |

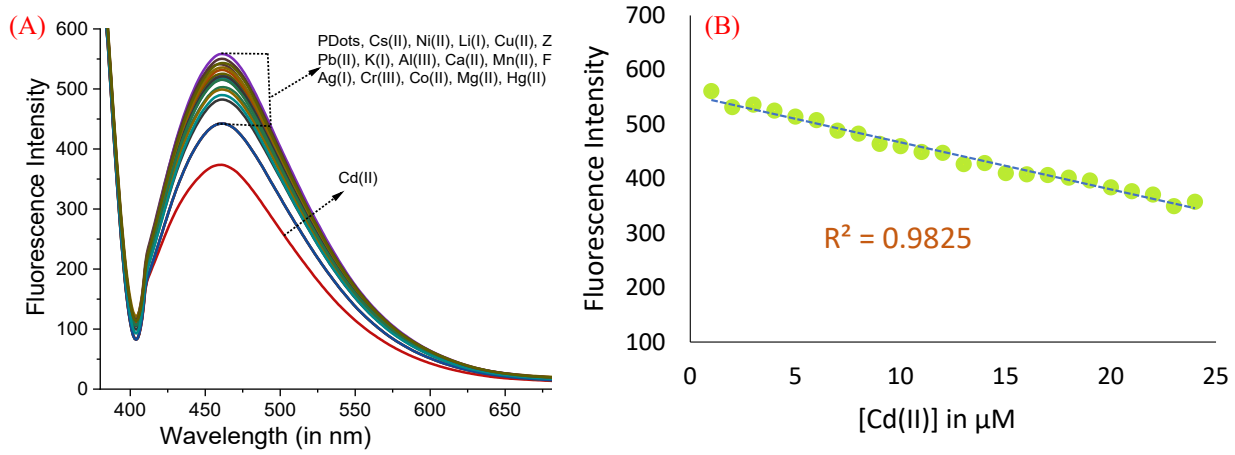


**Figure S2:** (A) Recognition studies of P.Dots in presence of various metal ions (Cs(II), Ni(II), Li(I), Cu(II), Zn(II), Pb(II), K(I), Al(III), Ca(II), Mn(II), Fe(III), Ag(I), Cr(III), Co(II), Mg(II), Hg(II)). and (B) Straight line plot of fluorescence intensity and concentration of Cd(II) ions.

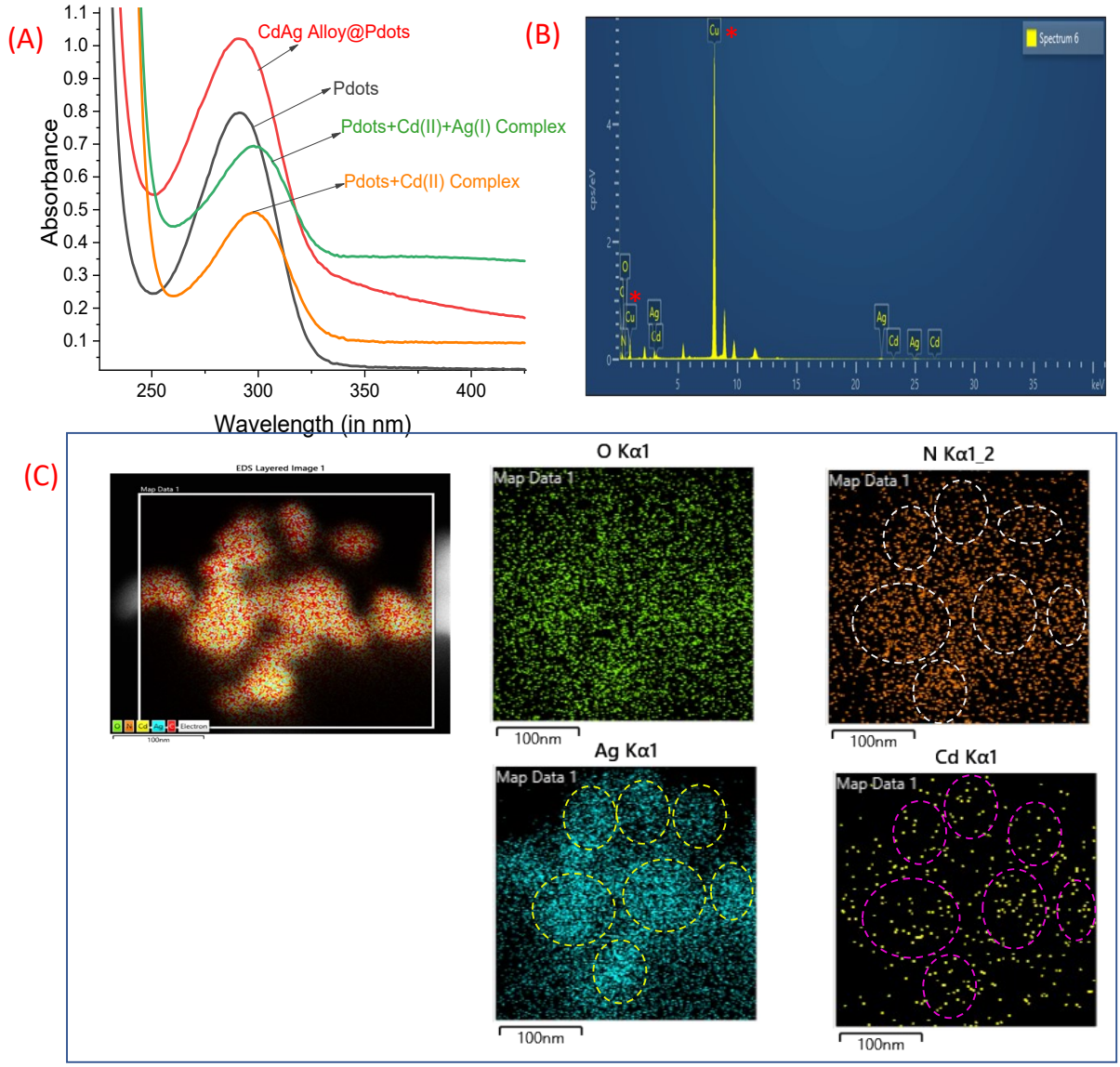


**Figure S3:** (A) UV- visible absorbance spectral profiles CdAg Alloy@Pdots in comparison with Pdots only, Pdots+Cd(II) comlex and Pdots+Cd(II)+Ag(I) complex. (B) EDX analysis of CdAgAlloy@Pdots showing presence of all elements, the peak corresponding to Cu mark with a star comes from the carbon coated copper grid used for STEM-EDX mapping. (C) STEM image of CdAgAlloy@Pdots and the elemental mapping of Oxygen, Nitrogen, Silver, and Cadmium respectively.

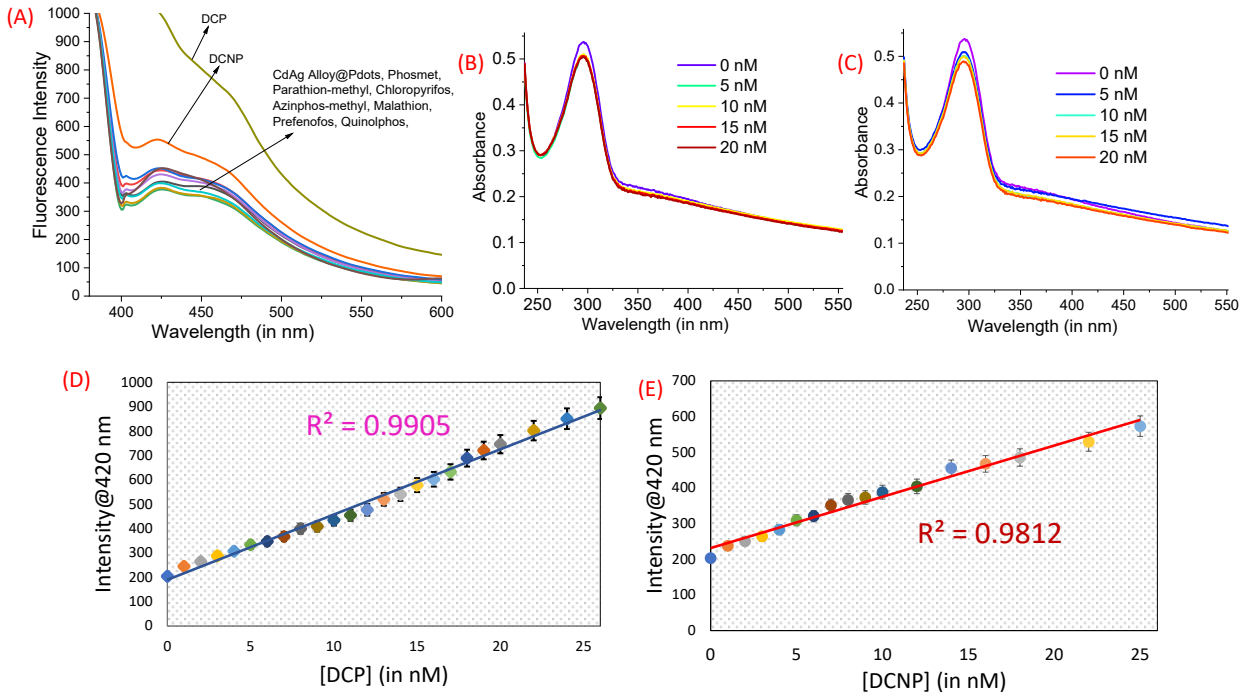


**Figure S4:** (A) Recognition studies of CdAg Alloy@Pdots in presence of different organophosphates by using Fluorescence spectrophotometer. UV-visible absorption Titration of CdAg Alloy@Pdots with increasing concentration of (B) DCP and (C) DCNP from 0 nM to 25 nM. (D) and (E) Straight line plot of fluorescence intensity with concentration of DCNP and DCP respectively.

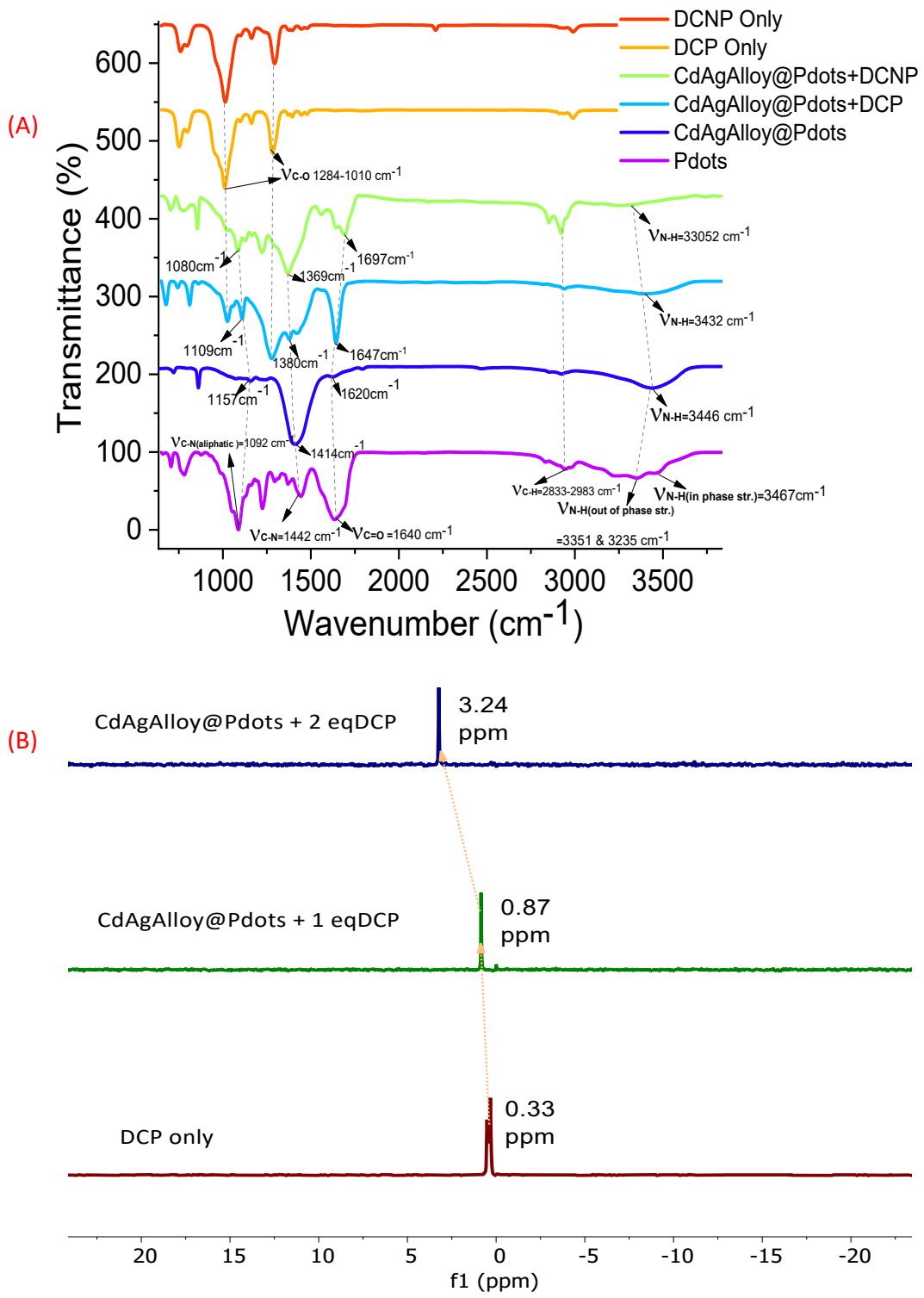


**Figure S5**: (A) Stacked FTIR spectra of complex CdAg Alloy@Pdots+DCP and CdAg Alloy@Pdots+DCNP in comparison with CdAg Alloy@Pdots, Pdots only, DCP only and DCNP

only. (B) $^{31}P$ NMR of CdAgAlloy@Pdots in presence of increasing equvalents of DCP recorded in $D_2O$ solvent.

.

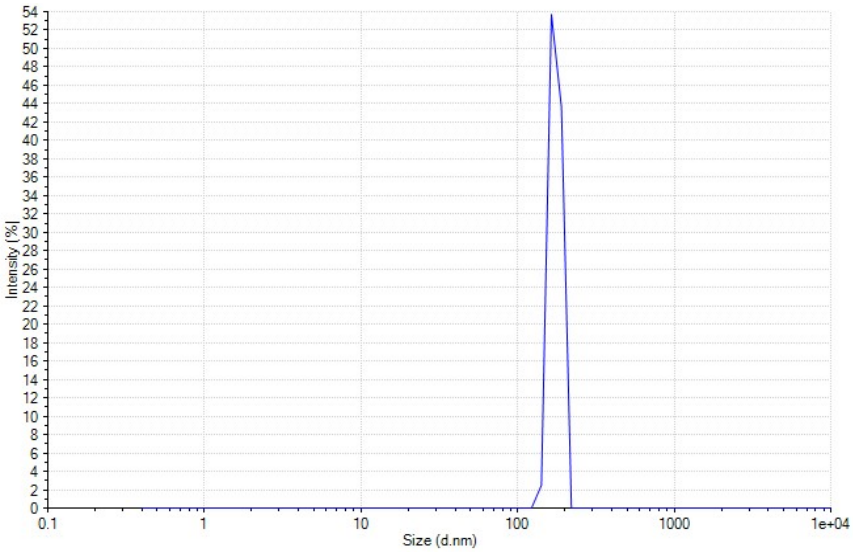


**Figure S6:** DLS histogram of CdAgAlloy@PDots+DCP shows average size in range of 124-130 nm.

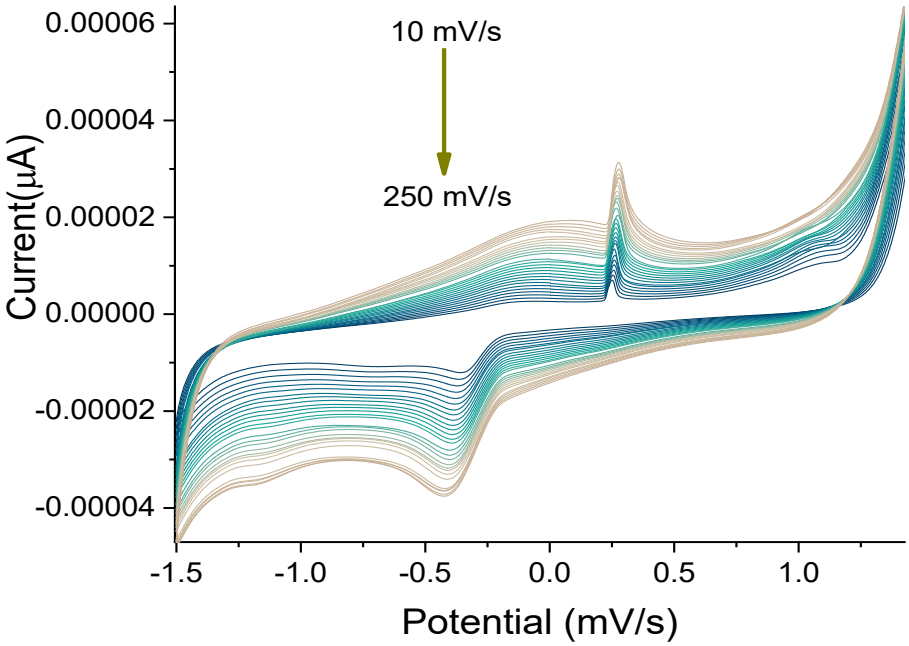

**Figure S7:** Scan rate study at different scan rate (10 mV/S to 250 mV/S) at concentration 22 nM of DCP.

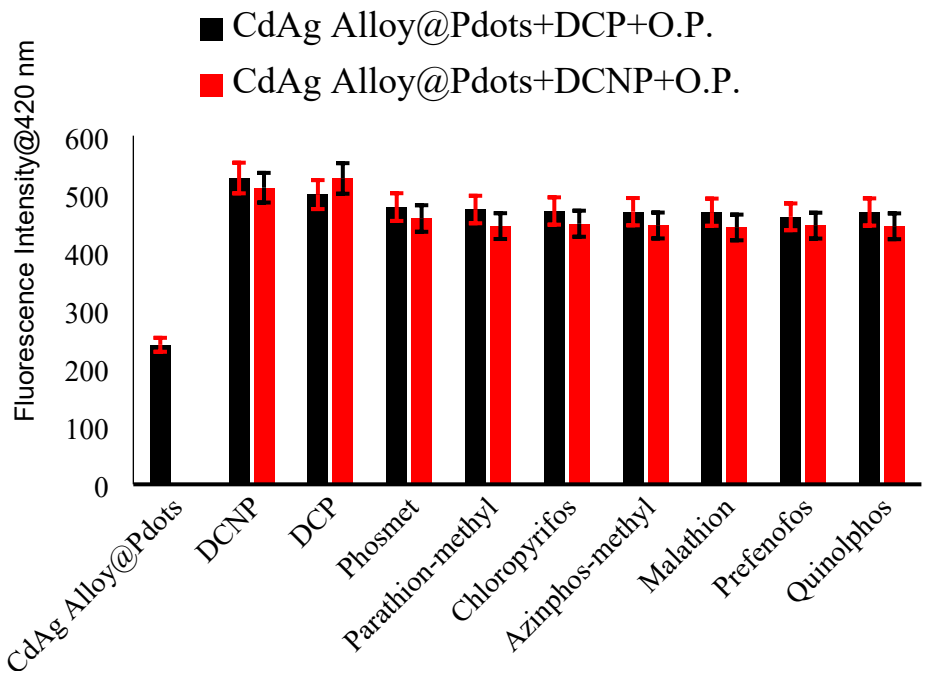


**Figure S8:** Bar graph showing interference studies of CdAgAlloy@Pdots complex with DCP and DCNP respectively, in presence of other phosphates.

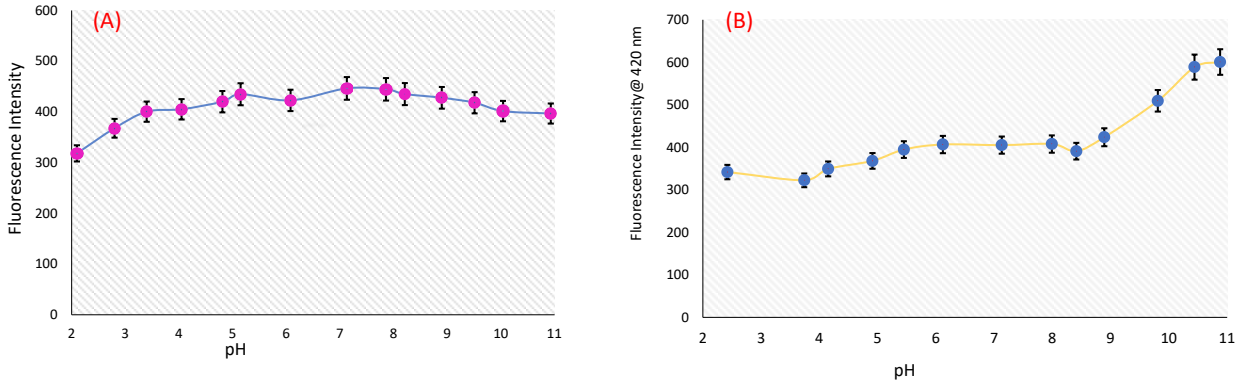


**Figure S9:** pH effect studies of (A) Pdots and (B) CdAg Alloy@Pdots in wide range of pH from 2-11.

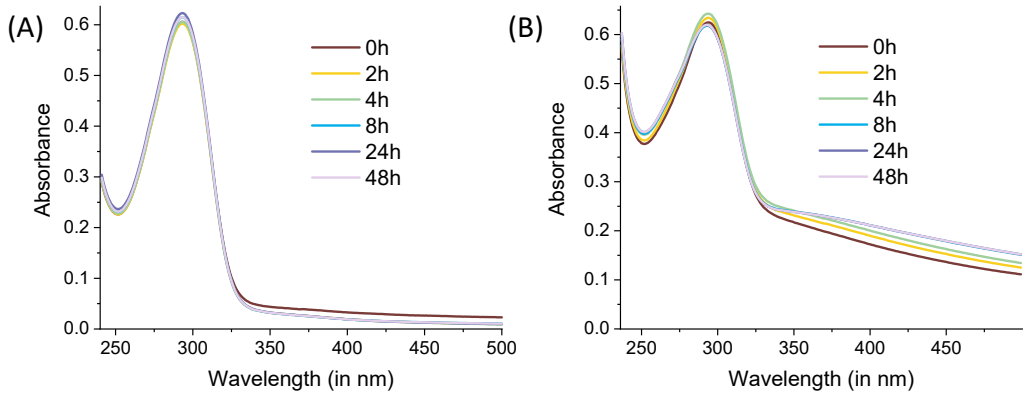


**Figure S10:** Absorption spectra of (A) Pdots and (B) CdAgAlloy@Pdots showing no remarkable change after 48h of low power UV-light irradiation.

**Table S2**: Comparison of LOD and studies with reported other sensing materials of DCP and DCNP.

| Entry | Probe | Analyte | Solvent | Response Type | LOD | Response Time | Application | Reference |
|---|---|---|---|---|---|---|---|---|
| **1.** | 4-diphenylamino-2-hydroxy benzaldehyde oxime (TPOD) | DCP | $CH_3CN$-$H_2O$ (4:6, v/v) | Fluorescence Ratiometric | 0.14 µM | 30 s | Vapor Phase | [1] |
| **2** | Naphthalimide-based-fluorescent probe | DCP | DMF | Fluorescence Enhancement | 5.5 nM | 300 s | Vapor Phase | [2] |
| **3** | Rhodamine-deoxylactum-based Fluorescent probe | DCP | DMF (3% $Et_3N$) | Fluorescence Enhancement | 9.66 nM | 30 s | Vapor Phase | [3] |
| **4** | Rhodamine based Probe | DCP | EtOH–$H_2O$ (1 : 1 v/v) | UV/Fluorescence Enhancement | - | - | - | [4] |
| **5** | Polymer fibers | DFP/DCP | MeOH/ $H_2O$ | UV/ Fluorescence, Ratiometric | 0.18 µM/ 0.16 µM | 20 s | Vapor Phase | [5] |

| | | | | | | | | |
|---|---|---|---|---|---|---|---|---|
| **6** | Binaphthol-Si Complex | DCP | DMF | Fluorescence Quenching | 0.0097mmol/L | 4 s | Vapor Phase | [6] |
| **7** | Azine based fluorescent probe | DCP | Acetonitrile/water (2:8) | Fluorescence Enhancement | 9.86 nM | 2 min. | Vapor Phase | [7] |
| **8** | PTS based Covalent assambly | DCP | Acetonitrile | Fluorescence Enhancement | 10.4 nM | 100 s | Vapor Phase | [8] |
| **9** | Heteroleptic Eu(III) Luminescent probes | DCP | MeCN | Luminescence Quenching | 10 ppb | 10 min. | Vapor Phase | [9] |
| **10** | Triazole-based Fluorescent probe | DNT/$H_2O_2$/DCP | THF | Fluorescence Quenching/ enhancement /ratiometric | - | 2 s | Vapor Phase | [10] |
| **11** | 1D photonic crystal (1D PC) films | DCP | - | Colorimetric | 8 ppm | - | Vapor Phase | [11] |
| **12** | BTCP Fluorescent probe | DCP | MeCN/ H2O (1/1, v/v,) | UV/ Fluorescence Enhancement | 15.8 nM | 10 s | Vapor Phase and Bioimaging | [12] |
| **13** | Benzothiazole-based Fluorescent Probe | DCP | MeCN | UV/ Fluorescence Enhancement | 0.186 µM | 6 s | Vapor Phase | [13] |
| **14** | 4H-1, 2, 4-triazole (TAZ)-based Polymeric Probe | DCP | THF | Fluorescence Quenching | 2.3 nM | 5 s | Vapor Phase | [14] |
| **15** | Polymeric Film | DCP/Ammonia | Water | Colorimetric and Absorbance shift | 18.4 µM/ 133µM | < 1 min. | Vapor Phase | [15] |
| **16** | CdAg Alloy@Pdots | DCP/DCNP | Water | Fluorescence Enhancement | 0.85 nM and 1.2 nM | 20 s | Vapor Phase | Present Work |

**References**

[1] S. S. Ali, A. Gangopadhyay, A. K. Pramanik, U. N. Guria, S. K. Samanta and A. K. Mahapatra, *Dyes and Pigments* 2019, 170, 107585.

[2] H. Xu, H. Zhang, L. Zhao, C. Peng, G. Liu and T. Cheng, *New J. Chem.,* 2020, **44**, 10713—10718

[3] G. Heo, R. Manivannan, H. Kim and Y.-A. Son, Dyes and Pigments 2019, **171**, 107712

[4] K. C. Beheraab and B. Bag, *Chem. Commun.,* 2020, **56**, 9308—9311

[5] F. W. Dagnaw, W. Feng and Q-H. Song, *Sensors & Actuators: B. Chemical* 2020, **318**, 127937

[6] X. Fenga, Y. Wangb, W. Fengc and Y. Peng, Chinese Chemical Letters 2020, **31**, 2960–2964

[7] R. Suhasini, R. Karpagam, K. Thirumoorthy and V. Thiagarajan, *Spectrochimica Acta Part A: Molecular and Biomolecular Spectroscopy* 2021, **263**, 120206

[8] B. Huo, M. Du, A. Shen, M. Li, Y. Lai, X. Bai, A. Gong and Y. Yang, *Anal. Chem.,* 2019, **91**, 10979−10983

[9] Z. Abbas, U. Yadav, R. J. Butcher and A. K. Patra, *J. Mater. Chem. C*, 2021, **9**, 10037–10051

[10] P. Zheng, A. Abdurahman, Z. Zhang, Y. Feng, Y. Zhang, X. Ai, F. Li and M. Zhang, *Journal of Hazardous Materials* 2021, **409**, 124500

[11] S-H. Jung, Y. J. Jung, B. C. Park, H. Kong, B. Lim, J. M. Park and H-I Lee, *Sensors and Actuators: B. Chemical* 2020, **323**, 128698

[12] L. Patraa, P. Ghoshb, S. Dasa, S. Gharamia, N. Murmub and T. K. Mondal, *Journal of Photochemistry & Photobiology A: Chemistry* 2020, **388**, 112188

[13] X. Hua, H. Zengb, T. Chenb, H-Q Yuanc, L. Zengb and G-M. Bao, *Sensors & Actuators: B. Chemical* 2020, **319**, 128282

[14] P. Zheng, A. Abdurahman, G. Liu, H. Liu, Y. Zhang and M. Zhang, *Sensors & Actuators: B. Chemical* 2020, **322**, 128611

[15] T. N. Annisa, S-H. Jung, M. Gupta, J. Y. Bae, J. M. Park and H-I Lee, *ACS Appl. Mater. Interfaces* 2020, **12**, 11055−11062